



# MODIFICATIONS TO THE IRON ABUNDANCE ALGORITHM BASED ON MOON MINERALOGY MAPPER ON-BOARD CHANDRAYAAN-1



M. Bhatt<sup>1</sup>, U. Mall<sup>1</sup>, C. Wöhler<sup>2</sup>, R. Bugiolacchi<sup>1</sup>, A. Berezhnoy<sup>3</sup> and A. Grumpe<sup>2</sup>



<sup>1</sup>Max Planck Institute for Solar System Research, 37191 Katlenburg-Lindau, Germany (bhatt@mps.mpg.de).

<sup>2</sup>Image Analysis Group, TU Dortmund University, 44227 Dortmund, Germany.

<sup>3</sup>Sternberg Astronomical Institute, Moscow State University, Moscow, Russia.

## Introduction

Several algorithms have been proposed to estimate FeO weight percent (wt.%) based on the 1- $\mu$ m absorption band parameters for the Clementine and telescopic datasets [e.g., 1–5]. Most of the empirical models relying on mineralogical measurement techniques are based on separating the space weathering effects from the mineralogical composition of the uppermost surface layer. Recently a new algorithm has been proposed in [6] based on the 2- $\mu$ m absorption parameters using the data from the infrared spectrometer SIR-2 [7] and the Moon Mineralogy Mapper (M<sup>3</sup>) [8] on-board Chandrayaan-1 [9]. In [6], the M<sup>3</sup> spectra were normalized to the reflectance at 1.5  $\mu$ m, but no further photometric or topographic correction was applied.

In this study, we have modified the FeO abundance estimation equation from [6] for M<sup>3</sup> data by applying photometric and topographic corrections. This modified algorithm is applied to the crater Tycho and its surrounding. We compare our results with the Clementine-based FeO wt.% map generated using the algorithm in [2] and the regression-based approach [10] relying on M<sup>3</sup> data.

## M<sup>3</sup>-based FeO abundance estimation algorithm

Based on the method in [11], the M<sup>3</sup> radiance data [12] have been photometrically and topographically corrected using the Hapke model [13] and the GLD100 [14], and a 20 pixels per degree global reflectance mosaic has been prepared. The 2- $\mu$ m band depth (BD2) vs. normalized continuum slope (CS2) relation has been derived according to [6] (Fig. 1b) from the calibration site (Fig. 1a). The slope coefficient derived from Fig 1b is used for computing an empirical calibration between the band parameters and laboratory FeO wt.% measurements [6]. The modified FeO content corresponds to:

$$FeO [wt.\%] = 70.028 \times (BD2 + 0.562 \times CS2) - 6.725 \quad (1)$$

Based on Eq. (1), we constructed a FeO map of the western lunar nearside region (40°W to 5°E and 55°S to 55°N). A second FeO map and a TiO<sub>2</sub> map were derived using [10], which is an extension of the regression-based approach [5] relying on Lunar Prospector elemental abundances [15] as a reference. The difference between the two constructed FeO maps is linearly correlated with the estimated TiO<sub>2</sub> content with a correlation coefficient of 0.82, leading to a TiO<sub>2</sub> corrected 2- $\mu$ m band based FeO abundance according to:

$$FeO_{corr} [wt\%] = FeO + 1.647 \times TiO_2 - 4.300 \quad (2)$$

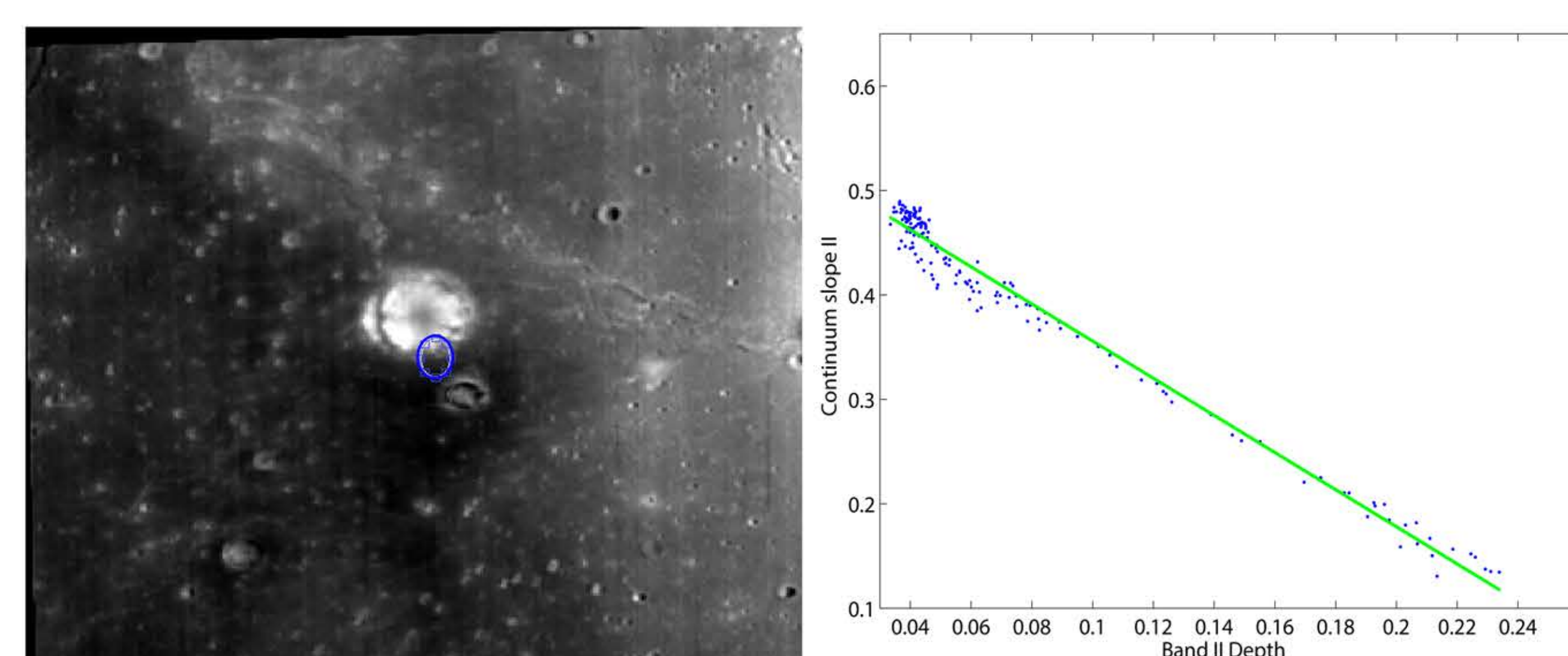
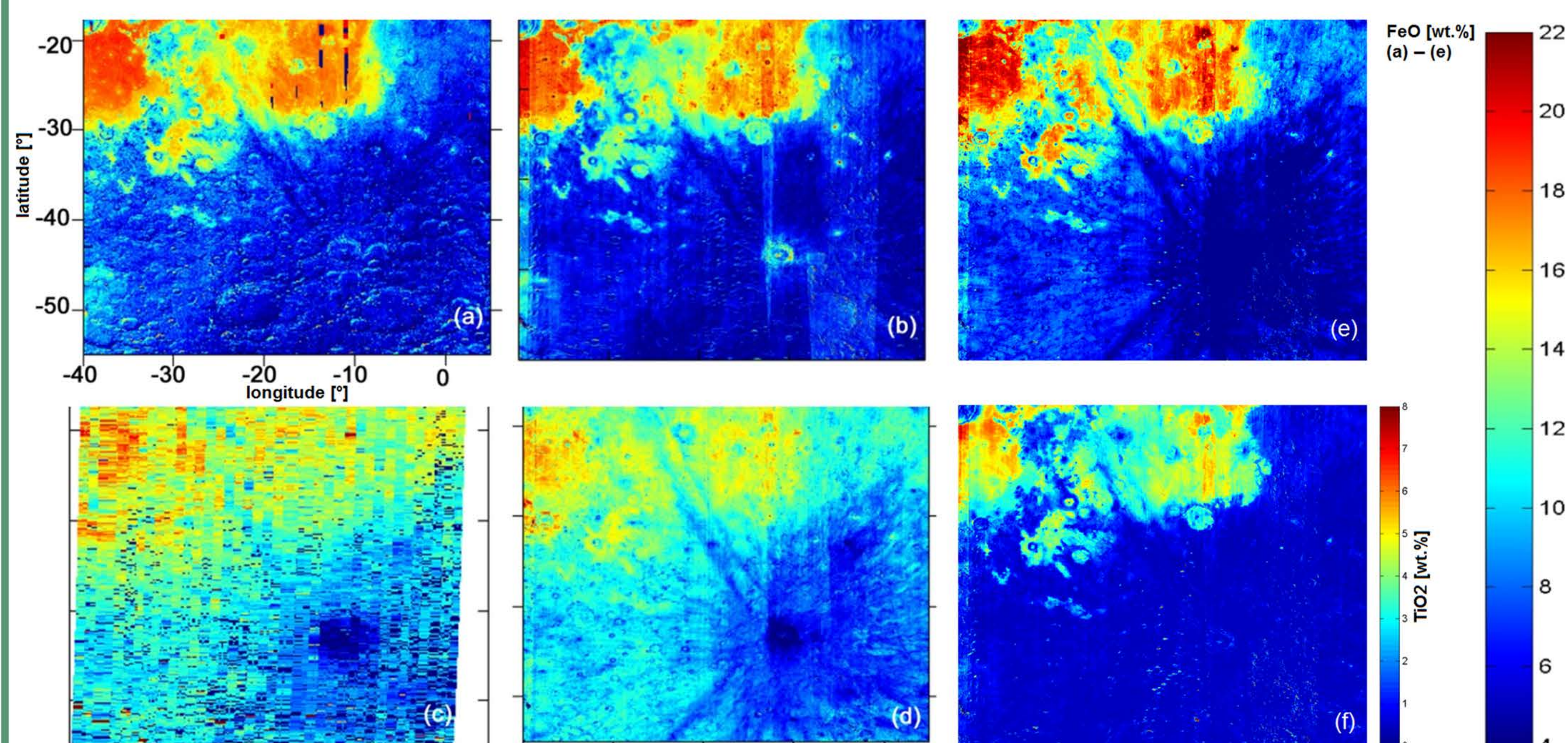


**Fig. 1:** Photometrically and topographically corrected M<sup>3</sup> 1579 nm reflectance mosaic of the region around crater Bonpand D (left) and correlation plot of the normalized continuum slope versus the 2- $\mu$ m absorption band depth (right). The band parameters are extracted from the reflectance spectra of the marked area on the southern crater rim.

## FeO abundance map of Tycho and surroundings



The FeO abundance estimated using [6] qualitatively shows the same trend as the FeO maps derived from Clementine data [2] and M<sup>3</sup> data [10]. The algorithm in [6] is less sensitive to the topography than the approach in [2]. Furthermore, the FeO map in Fig. 2d constructed based on the 2- $\mu$ m band parameters reveals stronger variations of the FeO abundances than the FeO maps in Fig. 2a and 2b. In the mare regions (Mare Humorum and Mare Nubium), Eq. (1) estimates 2–6 wt.% less FeO for mare regions than the methods in [2] and [10]. In the FeO map corrected for TiO<sub>2</sub> according to Eq. (2), the systematic deviations between the FeO estimation algorithm based on the 2- $\mu$ m band parameters alone and the approaches including the 1- $\mu$ m band parameters are reduced significantly.

**Fig. 2:** FeO abundance maps of the crater Tycho and its surroundings. (a) Clementine FeO map derived using [2]; M<sup>3</sup> FeO map using [10]; (c) SIR-2 FeO map derived using 39 equidistant tracks using equation (4) from [6]; (d) M<sup>3</sup> FeO map generated using Eq. (1); (e) M<sup>3</sup> FeO map corrected for TiO<sub>2</sub> using Eqs. (1) and (2); (f) M<sup>3</sup>-based TiO<sub>2</sub> map obtained using [10].

**Summary:** The FeO abundance estimation algorithm [6] based on the 2- $\mu$ m absorption band has been modified for photometrically and topographically corrected M<sup>3</sup> data. After applying the modified algorithm, the M<sup>3</sup> FeO abundance shows a better match with the FeO abundance estimated for SIR-2 data. Our comparative analysis of the Tycho region using three different algorithms shows qualitatively similar FeO variations. Taking into account the TiO<sub>2</sub> content reduces the systematic deviations between the 2- $\mu$ m band based FeO estimation algorithm and the approaches including the 1- $\mu$ m band parameters.

**References:** [1] Lucey P. G. et al. (1995), Science 268, 1150–1153; [2] Lucey P. G. et al. (2000) JGR 105, 20297–20306; [3] Le Mouéléc S. et al. (2000) JGR 105, 9445–9456; [4] Shkuratov Y. G. et al. (2005) PSS 53, 1287–1301; [5] Wöhler C. et al. (2011) PSS 59, 92–110; [6] Bhatt M. et al. (2012) Icarus 220, 54–60; [7] Mall U. et al. (2009) Current Science 96, 506–511; [8] Pieters C. M. et al. (2009) Current Science 96, 500–505; [9] Goswami J., Annadurai M. (2009) Current Science 96, 486–491; [10] Grumpe A. et al. (2012) Proc. 3rd Moscow Solar System Symp.; [11] Grumpe A., Wöhler C. (2011) Proc. 7th IEEE Int. Symp. Image and Signal Proc. and Anal., 609–614; [12] <http://pds-imaging.jpl.nasa.gov/volumes/m3.html>; [13] Hapke, B. (2002) Icarus 157, 523–534; [14] Scholten, F. et al. (2012) JGR 117, E00H17; [15] <http://www.mapaplanet.org/explorer/moon.html>.